

## ARTICLE

# Development of an inducible caspase-9 safety switch for pluripotent stem cell-based therapies

Chuanfeng Wu<sup>1</sup>, So Gun Hong<sup>1</sup>, Thomas Winkler<sup>1</sup>, David M Spencer<sup>2</sup>, Alexander Jares<sup>1</sup>, Brian Ichwan<sup>1</sup>, Alina Nicolae<sup>3</sup>, Vicky Guo<sup>1</sup>, Andre Larochelle<sup>1</sup> and Cynthia E Dunbar<sup>1</sup>

Induced pluripotent stem cell (iPSC) therapies offer a promising path for patient-specific regenerative medicine. However, tumor formation from residual undifferentiated iPSC or transformation of iPSC or their derivatives is a risk. Inclusion of a suicide gene is one approach to risk mitigation. We introduced a dimerizable-“inducible caspase-9” (iCasp9) suicide gene into mouse iPSC (miPSC) and rhesus iPSC (RhiPSC) via a lentivirus, driving expression from either a cytomegalovirus (CMV), elongation factor-1  $\alpha$  (EF1 $\alpha$ ) or pluripotency-specific EOS-C(3+) promoter. Exposure of the iPSC to the synthetic chemical dimerizer, AP1903, *in vitro* induced effective apoptosis in EF1 $\alpha$ -iCasp9-expressing (EF1 $\alpha$ )-iPSC, with less effective killing of EOS-C(3+)-iPSC and CMV-iPSC, proportional to transgene expression in these cells. AP1903 treatment of EF1 $\alpha$ -iCasp9 miPSC *in vitro* delayed or prevented teratomas. AP1903 administration following subcutaneous or intravenous delivery of EF1 $\alpha$ -iPSC resulted in delayed teratoma progression but did not ablate tumors. EF1 $\alpha$ -iCasp9 expression was downregulated during *in vitro* and *in vivo* differentiation due to DNA methylation at CpG islands within the promoter, and methylation, and thus decreased expression, could be reversed by 5-azacytidine treatment. The level and stability of suicide gene expression will be important for the development of suicide gene strategies in iPSC regenerative medicine.

*Molecular Therapy — Methods & Clinical Development* (2014) **1**, 14053; doi:10.1038/mtm.2014.53; published online 12 November 2014

## INTRODUCTION

Induced pluripotent stem cell (iPSC) technologies hold great promise for regenerative medicine, based on their unlimited self-renewal capabilities and ability to differentiate to cell types derived from all three embryonic germ layers.<sup>1–3</sup> The ethical and practical issues surrounding procurement of embryonic stem cells (ESCs) are avoided, as are issues with immune rejection of allogeneic ESC-derived tissues, if patient-specific autologous iPSCs are utilized instead. Recent studies have shown promising results for iPSC-based regenerative cell therapies in rodent models and large animal models.<sup>4–6</sup> However, there are serious concerns regarding the safety of administering tissue grafts derived from ESCs/iPSCs. Residual pluripotent cells, aberrant cells resulting arising due to inherent genetic instability in cells cultured *in vitro* long-term, or transformed cells resulting from insertional mutagenesis due to reprogramming or genetic correction approaches could all lead to tumor formation.<sup>7–9</sup> Aberrant integration of new cells into an organ could also result in toxicity, even without overt malignant transformation. Introduction of a “suicide gene” safety switch into iPSC-derived cells has been pioneered in somatic cell gene therapy applications and might permit on-demand ablation of iPSC-derived transplanted cells in the case of an adverse event.<sup>10–12</sup>

The prototypical suicide gene system used in clinical and experimental settings relies on the herpes simplex virus thymidine kinase

(HSV-TK) gene, with suicide gene-specific metabolism of the anti-viral prodrug, ganciclovir (GCV), to a toxic nucleoside analog by the herpes TK enzyme.<sup>11,13,14</sup> A number of studies have shown that introduction of HSV-TK into target cells via retroviral gene transfer permits efficient elimination of transduced cells, including lymphocytes, hematopoietic stem and progenitor cells, hepatocytes, and ESCs/iPSCs, following *in vitro* or *in vivo* exposure to GCV.<sup>11,15–24</sup> However, HSV-TK is a viral protein shown to be immunogenic *in vivo*, and can stimulate immune rejection of transduced cells even in the absence of GCV administration.<sup>25</sup> Moreover, mutations arising within the HSV-TK gene were shown to result in GCV resistance in some patients transplanted with allogeneic T cells containing the HSV-TK suicide gene.<sup>26</sup> Finally, GCV is a potent and clinically useful antiviral drug that is used to treat serious herpes virus infections, such as cytomegalovirus, and lifelong avoidance of the use of GCV as an antiviral in patients transplanted with HSV-TK-containing cells may not be possible, resulting in ablation even of normally functioning transplanted tissues were GCV to be administered.

Recently, an alternative suicide gene safety switch system that circumvents some of the limitations of the HSV-TK/GCV system has been developed.<sup>27</sup> The fusion “inducible Caspase-9” suicide gene (iCasp-9) was engineered by replacing the Caspase recruitment domain (CARD) of pro-apoptotic caspase-9 with a mutated (F36V) dimerizer drug-binding domain from the human FK506-binding

<sup>1</sup>Hematology Branch, National Heart, Lung, and Blood Institute, National Institutes of Health (NIH), Bethesda, Maryland, USA; <sup>2</sup>Bellicum Pharmaceuticals, Inc, Houston, Texas, USA; <sup>3</sup>Laboratory of Pathology, Center for Cancer Research, National Cancer Institute, National Institutes of Health, Bethesda, Maryland, USA. Correspondence: CE Dunbar (dunbar@nhlbi.nih.gov)

Received 4 September 2014; accepted 12 September 2014

protein (FKBP12). This fusion protein has extremely high (~0.1 nmol/l) affinity for small molecular chemical inducers of dimerization (CID), such as research-grade AP20187 or the clinical candidate dimerizer AP1903, which induce apoptosis via activation of caspase-9.<sup>28–30</sup> The iCasp-9 gene product consists of almost 100% unmodified human components, and is thus unlikely to be immunogenic,<sup>27</sup> and has not induced detectable immunity in preclinical or clinical studies to date. These dimerizers were designed specifically for FKBP12 binding, and have no other clinical utility, thus unwanted ablation of suicide gene-containing cells due to drug administration for other indications is not an issue with the iCasp-9 system. The safety and ablation efficacy of the iCasp-9/AP1903 approach was recently investigated in a pilot clinical trial. Therapeutically-relevant reduction but incomplete reduction of iCasp-9-containing allogeneic T cells responsible for graft-versus-host disease occurred following a single nontoxic dose of AP1903.<sup>27</sup> In this study, we investigate the utility of the iCasp-9 suicide gene system in ablating undifferentiated teratogenic iPSC cells with AP1903 *in vitro* and preventing or treating teratomas derived from iPSC *in vivo*, and analyze the impact of promoter strength, promoter specificity for pluripotent versus differentiated cells, and gene silencing on the use of this system as an iPSC safety switch.

## RESULTS

Lentivirus-mediated iCasp9 expression and AP1903 sensitivity in murine and rhesus iPSC *in vitro*

We generated GFP<sup>+</sup> murine iPSC (miPSC) from GFP transgenic mouse fibroblasts via standard methodology utilizing lentiviral vectors, and documented pluripotency as shown in Supplementary Figure S1. These miPSC were then transduced with lentiviral vectors expressing an iCasp9-2A peptide-human truncated CD19 (hΔCD19) transgene driven from either elongation factor-1  $\alpha$  (EF1 $\alpha$ ) or cytomegalovirus (CMV) constitutive promoters, or the EOS-C(3+) stem cell-directed promoter, as detailed in Figure 1a,b, to produce EF1 $\alpha$ -iCasp9, CMV-iCasp9, and EOS-C(3+)-iCasp9 miPSCs. The iCasp9 mRNA expression level in the miPSCs varied depending on the promoter, with EF1 $\alpha$  and EOS-C(3+) driving easily detectable iCasp9 mRNA expression, but almost undetectable iCasp9 mRNA in the CMV-iCasp9-miPSC (Figure 1c). We more quantitatively assessed transgene expression from the constructs via live immuno-staining and flow cytometry for hΔCD19 (Figure 1d,e), showing a similar expression hierarchy to the mRNA analysis, with a rank order of the EF1 $\alpha$ -iCasp9, then EOS-C(3+)-iCasp9, then CMV-iCasp9 for the mean fluorescent intensity of hΔCD19 staining in undifferentiated miPSCs (Figure 1e). Interestingly, only partially differentiated CMV-iCasp9-miPSC cells, as assessed morphologically *in situ* via live staining on the culture plates, showed any hΔCD19 staining (Figure 1d).

We evaluated the sensitivity of the iCasp9-miPSCs to AP1903 exposure *in vitro*. As shown in Figure 1e and Supplementary Figure S2, parental non-iCasp9 were not affected by AP1903 treatment, even at the top concentration of 100 nmol/l. In contrast, 24 hours post-10 nmol/l AP1903 exposure, greater than 90% of EF1 $\alpha$ -iCasp9-miPSC were Annexin V positive, and 70% of EOS-C(3+)-iCasp9-miPSCs underwent apoptosis (Supplementary Figure S2a). However, no concentration of AP1903 killed CMV-iCasp9-miPSCs efficiently. There was no obvious difference in cell survival at the different AP1903 dosages tested from 1 to 100 nmol/l for EF1 $\alpha$ -iCasp9-miPSC (Supplementary Figure S2b), but the higher dose (50–100 nmol/l) AP1903 treatment tended to be less effective for killing EOS-C(3+)-iCasp9-miPSCs (Supplementary Figure S2b), perhaps due to

saturation of limited amounts of iCasp9 with AP1903 and eventual inhibition of dimerization at higher dimerizer doses.

Nonhuman primates represent a valuable new preclinical model for development of iPSC therapies.<sup>6</sup> We generated iCasp9-expressing rhesus macaque iPSC (RhiPSC). Because RhiPSC are very sensitive to culture conditions and difficult to transduce with lentiviral vectors, we first isolated monkey skin fibroblasts and bone marrow mesenchymal stromal cells (MSCs), transduced them with the EOS-C(3+) or EF1 $\alpha$ -iCasp9-2A-hΔCD19 lentiviral vectors, and then enriched for hΔCD19-expressing cells via microbead selection (Figure 2a). We tested the sensitivity of these differentiated fibroblasts to AP1903 *in vitro*. The EF1 $\alpha$ -iCasp9 transduced fibroblasts stably expressed hΔCD19 and were sensitive to AP1903 (Supplementary Figure S3b). Both the GFP and hΔCD19 driven by EOS-C(3+) promoter could express in rhesus fibroblasts or MSC, indicating that expression from the EOS-C(3+) promoter is not rhesus ESC/iPSC-specific (Supplementary Figure S3a,b). Thus, we focused on the EF1 $\alpha$ -iCasp9-RhiPSC for subsequent analyses. As shown in Figure 2a, the EF1 $\alpha$ -iCasp9 rhesus fibroblasts were reprogrammed,<sup>6</sup> and were pluripotent, karyotypically normal, and hΔCD19-positive (Supplementary Figure S3c,d and Figure 2d). These cells were very sensitive to AP1903 *in vitro*, with complete cell death of EF1 $\alpha$ -iCasp9-RhiPSC 24 hours following exposure to 10 nmol/l AP1903 (Figure 2c).

Impact of the iCasp9/AP1903 suicide gene system on teratoma formation and growth *in vivo*

Prevention of teratoma or other tumor formation *in vivo* is the primary justification for inclusion of a suicide gene in iPSC. Because AP1903-mediated *in vitro* killing of EF1 $\alpha$ -iCasp9 miPSC was most robust, we focused on teratoma studies utilizing this construct. As shown in Figure 3a, mice were injected subcutaneously or intramuscularly with EF1 $\alpha$ -iCasp9 miPSC or non-iCasp9 miPSC under a number of different AP1903 exposure conditions. Rapid teratoma formation was observed in mice injected with EF1 $\alpha$ -iCasp9 (Figure 3a) or non-iCasp9 miPSC (Supplementary Figure S4a) in the absence of AP1903 administration. In contrast, teratoma formation was significantly delayed in mice receiving EF1 $\alpha$ -iCasp9 miPSC exposed *in vitro* to 10 nmol/l AP1903 for 4 hours prior to implantation, with 50% of the recipient mice remaining teratoma-free for up to 400 days.

We also studied the impact of administration of AP1903 *in vivo*. In a pilot study shown in Supplementary Figure S4a, mice given a single dose of 1 mg/kg AP1903 on the day of EF1 $\alpha$ -iCasp9 miPSC implantation had delayed teratoma growth compared to no treatment with AP1903, but required euthanasia by day 60 since teratoma size reached 2 cm. We then treated animals with AP1903 5 mg/kg/day for 5 days beginning coincident with miPSC injection, and did observe significant delay of tumor growth compared to the saline-treated control group ( $P = 0.0009$ ) (Figure 3a). When initiation of AP1903 at either 1 mg/kg as a single dose (Supplementary Figure S4a) or 5 mg/kg per day for 5 days (Figure 3a) was delayed until tumors were already palpable, 1 week following miPSC injection, there was no apparent inhibition of tumor growth (Figure 3a and Supplementary Figure S4a). Histologically, we did not see differences in teratoma morphology in terms of germ layer and mature tissue composition between the different treatment groups; all three germ layers were found in the teratomas at the endpoints (Figure 3b and Supplementary Figure S4b), and robust vessel formation was observed in teratomas from all different groups which indicated that AP1903 diffusion within the tumor through capillaries should be sufficient (Supplementary Figure S6).

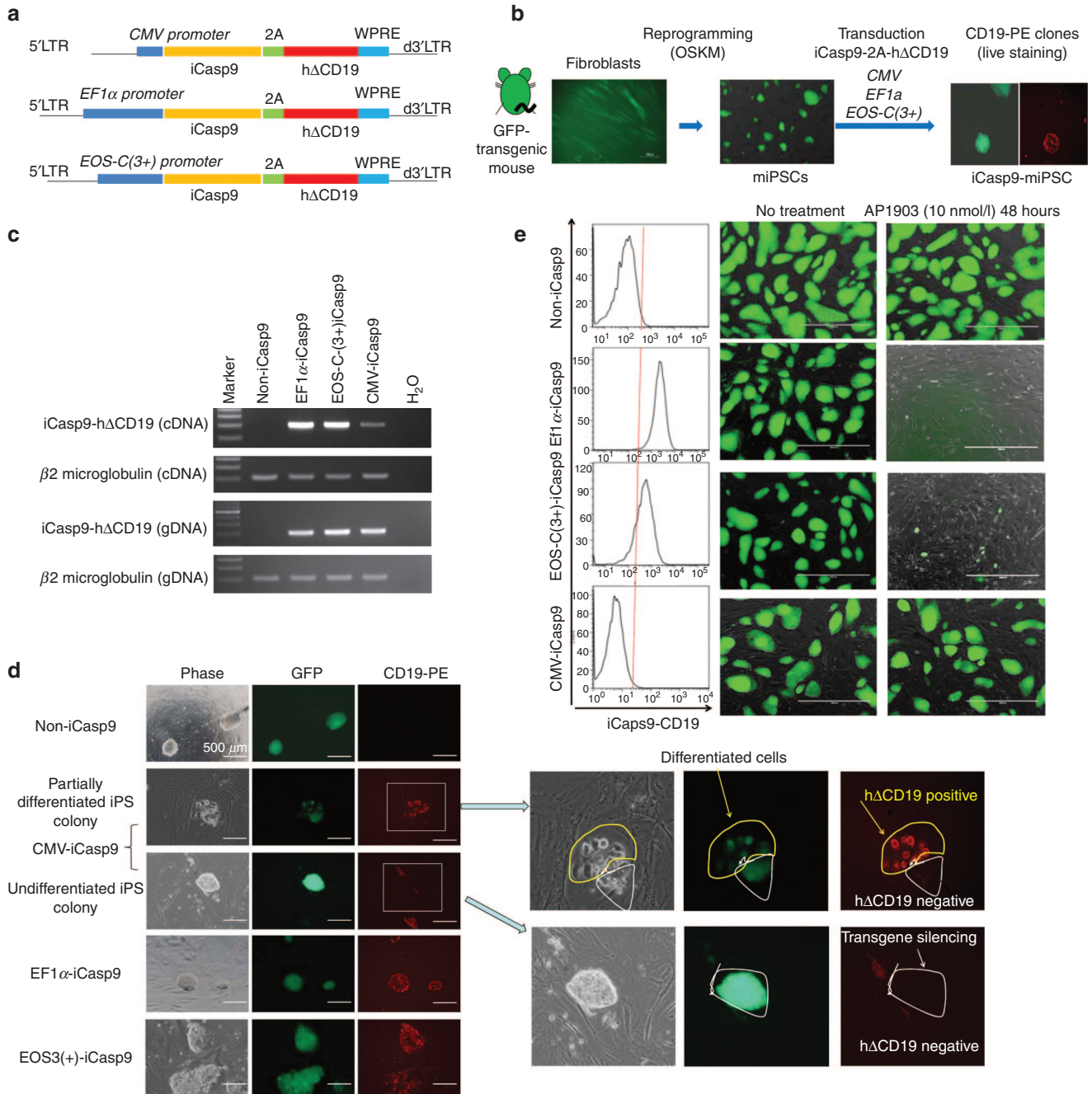


**Figure 1** Generation of iCasp9-expressing miPSC and efficacy of AP1903 killing *in vitro*. (a) Schematic of the lentiviral vectors, consisting of CMV, EF1α, or EOS-C(3+) promoters driving iCasp9 linked via a 2A peptide to the human truncated CD19 marker gene (hΔCD19). (b) Schematic of iCasp9 miPSC generation. (c) PCR for vector DNA or mRNA in miPSC clones transduced with the CMV, EF1α, or EOS-C(3+)-iCasp9-hΔCD19 vectors. (d) Live immunofluorescent staining and microscopic analysis for GFP (GFP-transgenic cells utilized for miPSC generation) and hΔCD19 marker gene expression in CMV, EF1α and the EOS-C(3+)-iCasp9-hΔCD19 miPSC clones grown on MEF supportive layers (GFP negative). Note that the CMV-iCasp9-hΔCD19 clones demonstrated lack of hΔCD19 transgene expression in undifferentiated colonies, but morphologically differentiating cells on the edge of colonies were CD19-PE positive (right enlarged panels). (e) hΔCD19 expression on miPSC transduced with the iCasp9-hΔCD19 vectors measured by flow cytometry (left panel), and iCasp9/AP1903-induced killing of cells following *in vitro* exposure to 10 nmol/l AP1903.

RhiPSCs were also studied *in vivo* in limited numbers of mice. Although teratoma growth from RhiPSC was slower than from miPSC, similar to the miPSC results, coincident treatment with AP1903 seemed to delay teratoma formation, but treatment beginning a week after RhiPSC implantation was not as effective (Supplementary Figure S4c,d).

We also developed another *in vivo* iPSC teratoma model to assess whether widespread intravenously disseminated pluripotent

cells could engraft and be impacted by AP1903 treatment. When three million miPSCs were injected intravenously, mice developed weight loss and eventually respiratory failure, with widespread teratoma structures filling the lungs and other vital organs including the kidneys (Figure 3d,e). We used this model to test the EF1α-iCasp9/AP1903 suicide system ablation efficiency *in vivo*. As shown in Figure 3c, the nontreated mice ( $n = 5$ ) died at day 15–28 post-miPSC intravenous injection, with lengthened survival in the group

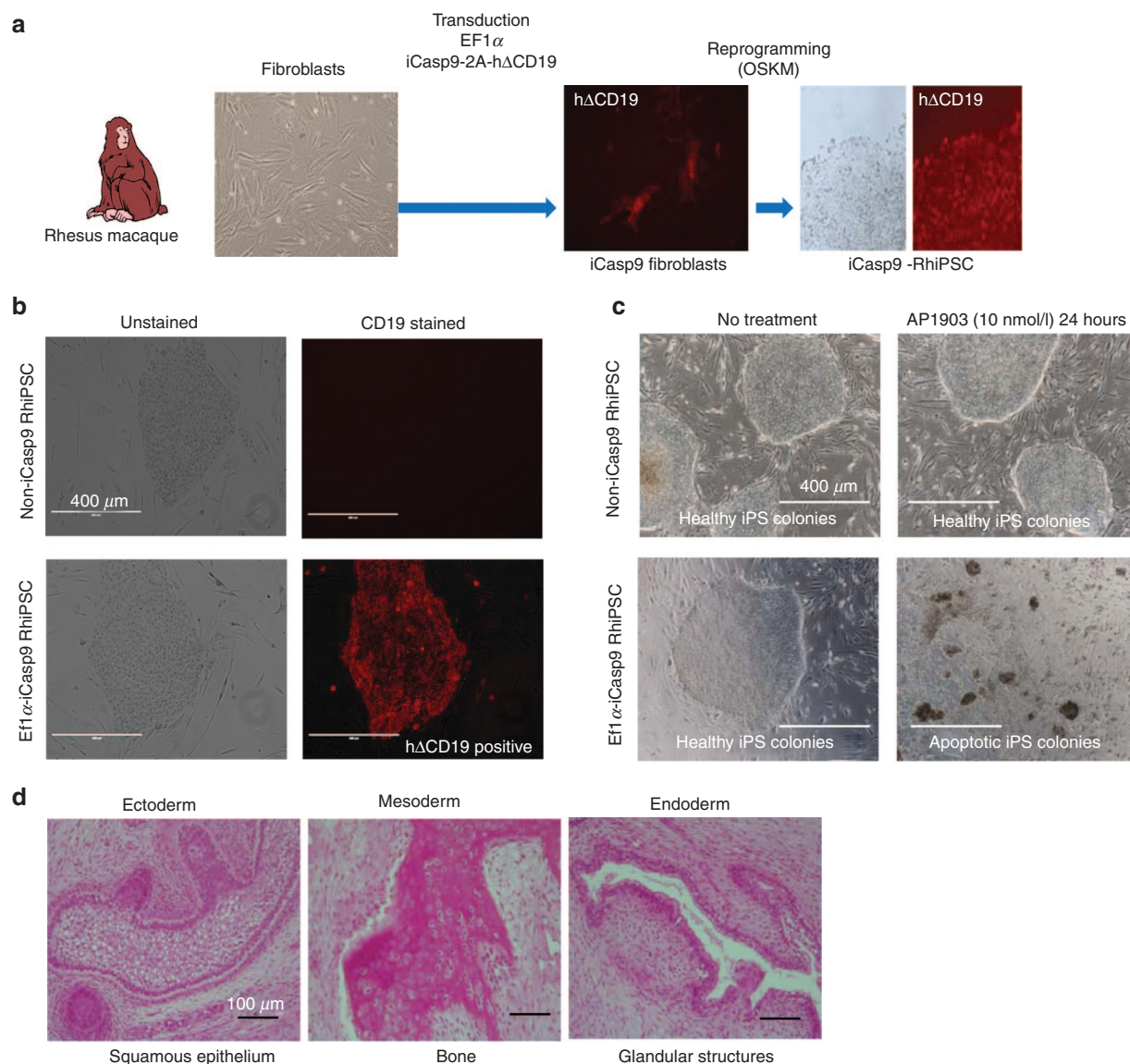


**Figure 2** Generation of iCasp9-expressing RhiPSC and efficacy of AP1903 killing *in vitro*. **(a)** Schematic showing generation of EF1 $\alpha$ -iCasp9-h $\Delta$ CD19-RhiPSC from monkey skin fibroblasts. **(b)** Live immunostaining with anti-CD19-PE of EF1 $\alpha$ -iCasp9-RhiPSC. **(c)** Exposure of EF1 $\alpha$ -iCasp9-h $\Delta$ CD19-RhiPSC to AP1903 (10 nmol/l) treatment *in vitro*. **(d)** Demonstration of teratoma formation from EF1 $\alpha$ -iCasp9-RhiPSC *in vivo* in NSG mice, with all three germ layers present.

treated with AP1903 beginning a week after miPSC administration ( $P = 0.0034$ ,  $n = 5$ ), and much longer survival in the group receiving AP1903 beginning on the day of miPSC administration ( $P = 0.0169$ ,  $n = 3$ ). These mice were still alive at 192 days follow-up.

#### Silencing of EF1 $\alpha$ -iCasp9 during iPSC differentiation *in vitro* and *in vivo*

To investigate why AP1903 was not fully effective *in vivo*, particularly for established teratomas, we analyzed h $\Delta$ CD19 expression as a surrogate for iCasp9 expression in explanted teratomas arising in AP1903-treated mice. Unlike *in vitro*, h $\Delta$ CD19 expression was barely detectable in the differentiated cells present in explanted teratomas that result from miPSC implantation, with or without AP1903 treatment (Figure 4a), and was very low in teratomas arising in mice transplanted with RhiPSC (Figure 4b). Actual AP1903 sensitivity could not be assessed since the explanted teratoma cells could not be passaged *in vitro*, but our *in vitro* AP1903 sensitivity assays showed that h $\Delta$ CD19 expression predicts sensitivity to AP1903 killing.

We differentiated EF1 $\alpha$ -iCasp9-RhiPSC *in vitro* to embryoid bodies (EBs), and monitored transgene expression. There was rapid downregulation of the transgene during differentiation, with only 1.8% residual h $\Delta$ CD19 expression by day 17, with the most marked drop occurring during the first 10 days (Figure 4c). iCasp9 mRNA levels also dropped significantly by EB day 10, and then stabilized (Figure 4d). Since EBs produce very heterogeneous differentiated cell types, we differentiated EF1 $\alpha$ -iCasp9-RhiPSC to a homogeneous population of CD73<sup>+</sup> mesenchymal stromal cells and analyzed transgene expression (Figure 4e). Early passage (P2) EF1 $\alpha$ -iCasp9-RhiPSC-derived MSC had higher h $\Delta$ CD19 expression compared to later passages (P4 and P5). The pattern of mRNA expression levels was consistent with the h $\Delta$ CD19 expression pattern (Figure 4f). We treated the passage 4 RhiPSC-derived MSCs with AP1903 (10 nmol/l), and dead cells floating after 4 hours expressed h $\Delta$ CD19 while remaining, viable, attached MSC cells were dim/negative for h $\Delta$ CD19 expression (Figure 4g).

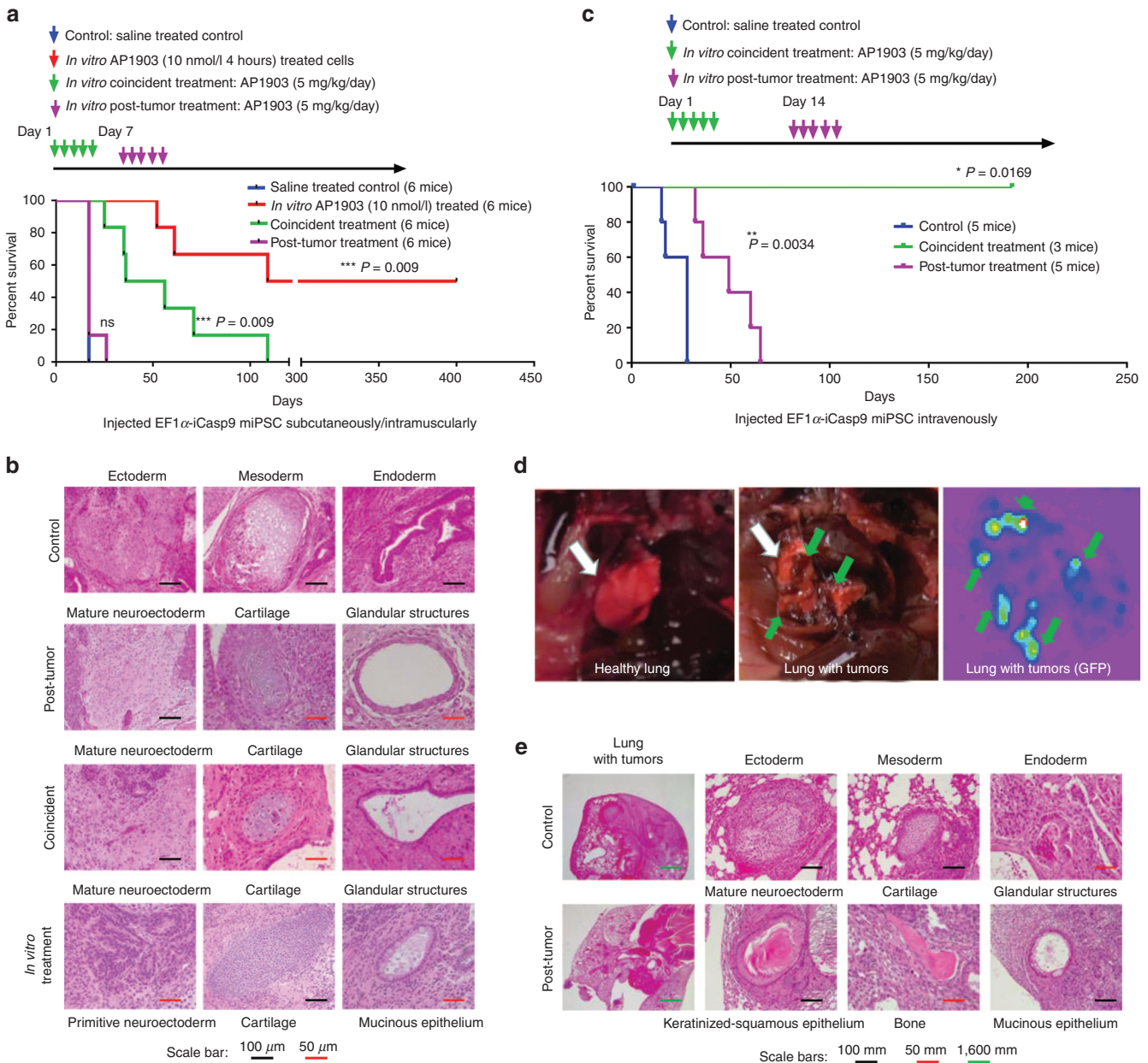


**Figure 3** Teratoma prevention or treatment with AP1903 in miPSC tumor models. **(a)** EF1 $\alpha$ -iCasp9 miPSCs were subcutaneously/intramuscularly injected into NSG mice. Schematic of treatment conditions and Kaplan–Meier survival curves for four groups of recipient NSG mice are shown: Positive control-EF1 $\alpha$ -iCasp9-h $\Delta$ CD19 miPSC with saline treatment (blue), *in vitro*-treatment of EF1 $\alpha$ -iCasp9-h $\Delta$ CD19 miPSC with AP1903 (10 nmol/l) for 4 hours *in vitro* just prior to injection of cells into NSG mice (red), Coincident-implantation of EF1 $\alpha$ -iCasp9-h $\Delta$ CD19 miPSC immediately followed by first dose of intravenous AP1903 (5 mg/kg/day, continued for a total of 5 days) (green), post-tumor treatment-AP1903 (5 mg/kg/day for 5 days) begun on day 7 and continuing through day 12 following implantation of EF1 $\alpha$ -iCasp9-h $\Delta$ CD19 miPSC, at time tumors already palpable (purple). The endpoint requiring euthanasia was a teratoma diameter of 2 cm. **(b)** Teratoma histology from tumors at the time of euthanasia, corresponding to groups in panel a. **(c)** EF1 $\alpha$ -iCasp9-h $\Delta$ CD19 miPSC were administered intravenously instead of subcutaneously, to model widespread hematogenous spread of teratoma-initiating miPSC. Schematic of treatments and Kaplan–Meier survival curves for three groups of recipient NSG mice: Positive control-EF1 $\alpha$ -iCasp9-h $\Delta$ CD19 miPSC with saline treatment (blue), Coincident-i.v. injection of EF1 $\alpha$ -iCasp9-h $\Delta$ CD19 miPSC immediately followed by first dose of intravenous AP1903 (5 mg/kg/day, continued for a total of 5 days) (green), post-tumor treatment-AP1903 (5 mg/kg/day for 5 days) begun on day 14 following i.v. injection of EF1 $\alpha$ -iCasp9-h $\Delta$ CD19 miPSC (purple). Mice were sacrificed when tumor size or overall clinical state met protocol-defined pre-morbidity criteria. **(d)** Macroscopic lung tumors in mice at the time of euthanasia from the control group in panel c. White arrow indicates healthy lung, and green arrows indicate macroscopic GFP<sup>+</sup> lung nodules (Carestream Xtreme GFP imaging shown in right panel). **(e)** Lung teratoma histology at the endpoints corresponding to panel c. All three germ layers were found in the teratomas.

#### Effects of EF1 $\alpha$ promoter CpG methylation on EF1 $\alpha$ -iCasp9 silencing during iPSC differentiation

One possible mechanism for transgene silencing is promoter DNA methylation. As shown in Figure 5a, the EF1 $\alpha$  promoter contains CpG islands; particularly a 200-bp region with more

than 70% GC content (Figure 5a, third panel). We analyzed the methylation status of the two CpG-rich EF1 $\alpha$  promoter regions (CpG island #1 and CpG island #2, shown in Figure 5a bottom panel) in teratoma cells explanted from mice in different treatment groups. As shown in Figure 5b, the methylation levels in

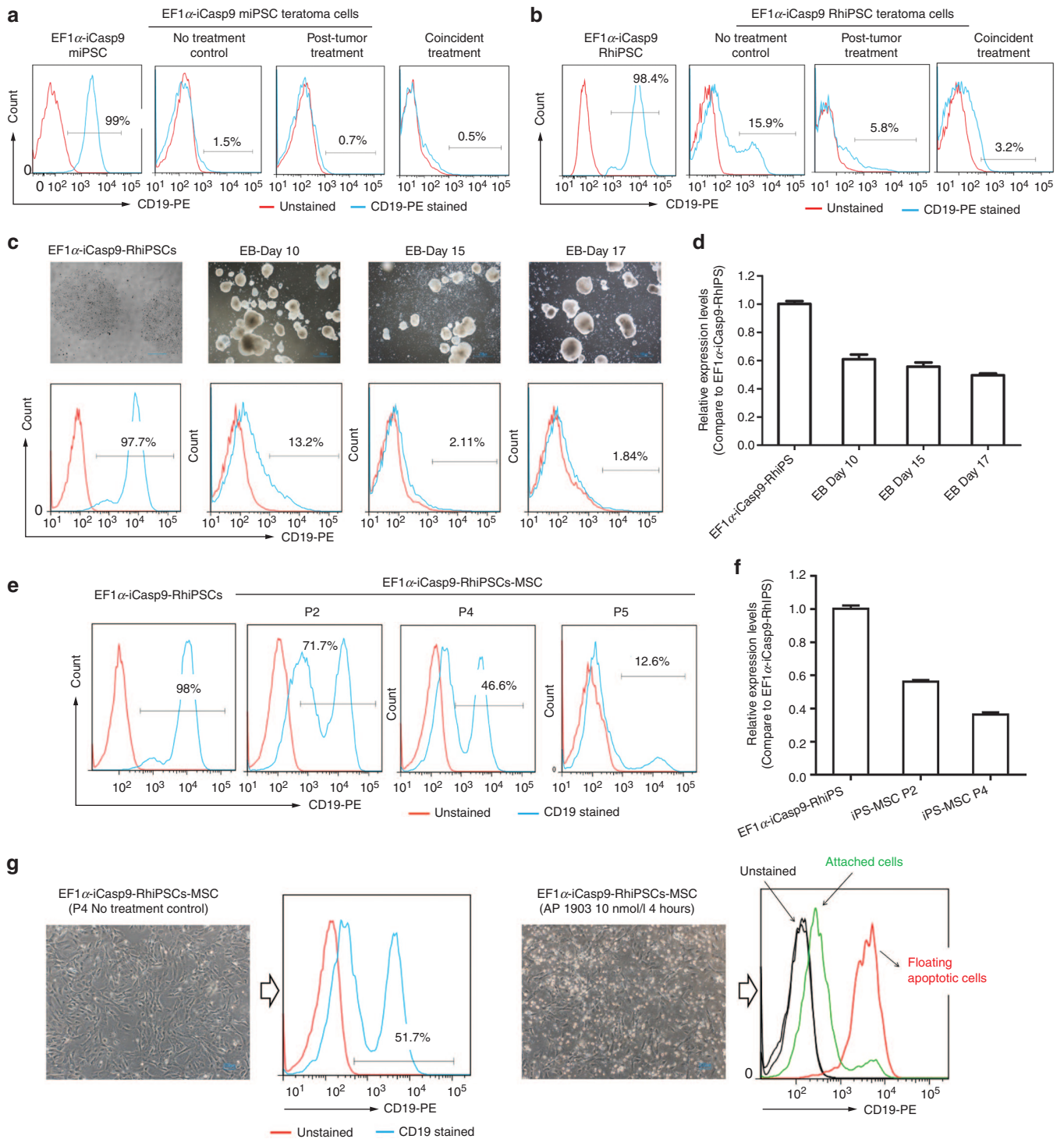


**Figure 4** EF1 $\alpha$ -iCasp9-h $\Delta$ CD19 silencing during iPSC differentiations *in vivo* and *in vitro*. **(a)** Flow cytometric analysis of the level of h $\Delta$ CD19 expression in cells explanted from endpoint miPSC teratomas arising in the NSG mice in the different treatment groups corresponding to Figure 3a (right panel), as compared to expression in the starting EF1 $\alpha$ -iCasp9-h $\Delta$ CD19 miPSC (left panel). **(b)** h $\Delta$ CD19 expression in cells explanted from RhiPSC endpoint teratomas from different NSG treatment groups (corresponding to Supplementary Figure S4c)(right panel), as compared to expression in the starting EF1 $\alpha$ -iCasp9-h $\Delta$ CD19-RhiPSC (left panel). **(c)** h $\Delta$ CD19 expression in EB differentiation cultures over time as compared to expression in the starting EF1 $\alpha$ -iCasp9-h $\Delta$ CD19-RhiPSC. **(d)** *iCasp9-hΔCD19* expression at the mRNA level in the EB culture overtime as compared to expression in the starting EF1 $\alpha$ -iCasp9-h $\Delta$ CD19-RhiPSC. **(e)** h $\Delta$ CD19 expression in different passages of iCasp9-h $\Delta$ CD19-RhiPSC-derived MSC compared to the starting iCasp9-h $\Delta$ CD19-RhiPSC. **(f)** *iCasp9-hΔCD19* expression at the mRNA level in the different passages of iCasp9-h $\Delta$ CD19-RhiPSC-derived MSC cells. **(g)** The sensitivity of the iCasp9-h $\Delta$ CD19-RhiPSC-derived passage 4 MSC to AP1903(10 nmol/l). The cells with high residual iCasp9-h $\Delta$ CD19 expression immediately came off the dish and began floating and dying, compared to the low/dim iCasp9-h $\Delta$ CD19 cells that remained attached and viable 4 hours after treatment.

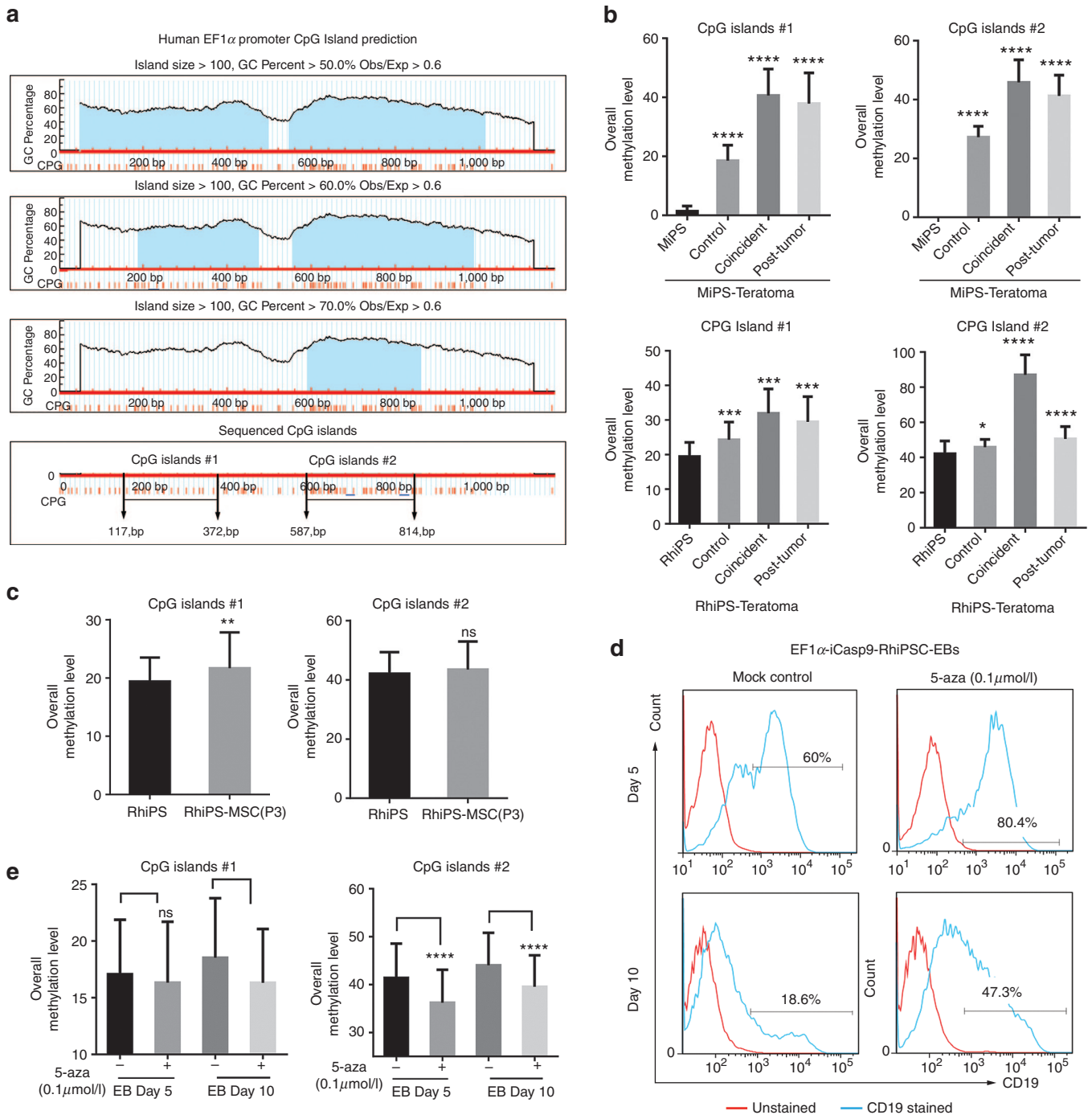


**Figure 5** Analysis of promoter methylation in EF1 $\alpha$ -iCasp9-h $\Delta$ CD19 iPSC and their differentiated derivatives. **(a)** CpG Island prediction for the human EF1 $\alpha$  promoter. The upper three panels show two CpG islands regions defined based on GC content. CpG island #1 (23 CpG sites) and island #2 (32 CpG sites) were analyzed via bisulfate sequencing (bottom panel) in all the samples described in Figure 5b,c,e. **(b)** The CpG methylation levels (the average of the methylation percentage of all CpG sites, mean  $\pm$  SEM) in both CpG islands of the teratoma cells were significantly higher than the preimplantation parental miPSCs or RhiPSCs (Unpaired  $t$ -test). **(c)** The CpG methylation levels in CpG island # 1 in RhiPSC-derived MSC (passage 3) were higher than in the parental RhiPSCs, while no significant difference was found in CpG island # 2 between the RhiPSC-MSC (P3) and the parental RhiPSCs (Unpaired  $t$ -test). **(d)** Downregulation of iCasp9-h $\Delta$ CD19 expression in embryoid bodies (EB) during *in vitro* differentiation from RhiPSC was partially restored by exposure to 5-azacytidine (0.1  $\mu$ mol/l), at two time points postdifferentiation induction (days 5 and 10). **(e)** The CpG methylation levels in the 5-aza treated EBs at day 10 were significantly lower than in the EBs without 5-aza exposure in both CG islands (Paired  $t$ -test). ns:  $P > 0.05$ , \* $P \leq 0.05$ , \*\* $P \leq 0.01$ , \*\*\* $P \leq 0.001$ , and \*\*\*\* $P \leq 0.0001$ .

both CpG islands from the teratoma cells were much higher than in both preimplantation parental miPSCs and RhiPSCs. The teratoma cells explanted from the coincident AP1903 treatment group had the highest methylation levels compared to the

control and post-tumor treatment groups. We also examined EF1 $\alpha$  promoter methylation in the RhiPSC-derived differentiated MSC. The methylation level in the EF1 $\alpha$  promoter CpG island #1 was significantly higher in the RhiPSC-derived MSCs than in the

parental RhiPSC; however, there was no significant difference in methylation at CpG island #2 (Figure 5c).

We attempted to rescue or maintain transgene expression by treatment with DNA methylation inhibitor, 5-azacytidine (5-aza), added during EB differentiation. h $\Delta$ CD19 expression was higher in the EB cultures treated with 5-aza (0.1  $\mu$ mol/l) compared to the untreated cells (Figure 5d), while the 5-aza treatment did not change the percentage of the h $\Delta$ CD19 positive cells in RhiPSC, but with an increase of expression density (Supplementary Figure S5). Bisulfate sequencing of the EF1 $\alpha$  promoter demonstrated lower methylation levels of CpG islands in EBs treated with 5-aza than in the EBs without 5-aza treatment (Figure 5e). These results indicate that EF1 $\alpha$  promoter CpG islands methylation may be responsible for iCasp9-h $\Delta$ CD19 silencing in cells derived from iPSC *in vitro* and *in vivo*.

## DISCUSSION

A major hurdle in the clinical development of first ESC and now iPSC has been concern regarding the serious risks inherent in delivering cell products derived from pluripotent stem cells.<sup>31</sup> ESC and iPSC are defined by their ability to form teratomas consisting of all three germ layers, and there is potential for residual pluripotent cells remaining in a differentiated cell product to form a teratoma after transplantation. Teratomas generally grow slowly and do not metastasize, however the presence of a teratoma in the heart, brain, eye, or another constrained and/or nonaccessible location would be very problematic. As few as two murine ESC mixed into a differentiated cell population formed teratomas in nude mice.<sup>32</sup> Autologous iPSC delivered into an immunocompetent nonhuman primate required delivery of millions of immature cells to form teratomas, but none the less, any residual undifferentiated cells do represent a risk.<sup>6</sup> Several murine ESC therapeutic models documented the risk of teratoma formation even with administration of apparently fully differentiated cells.<sup>33,34</sup>

Even in the absence of residual undifferentiated pluripotent cells, abnormal or unregulated proliferation of partially differentiated cells could be problematic. A recent report documented the presence of neural-stem cell derived tumors in a patient injected with fetal neural stem cells.<sup>35</sup> In addition, there are concerns that pluripotent cells and their progeny are particularly prone to additional genetic damage, resulting in malignant transformation. Genetic correction of iPSC with integrating vectors or even off-target effects of promising site-selective methodologies such as transcription activator-like effector nucleases (TALENs) or zinc finger nucleases could also result in tumorigenic genotoxicity.<sup>36</sup> Finally, even differentiated cells may cause toxicity if they localize incorrectly or do not integrate correctly with their microenvironment, for instance causing arrhythmias in the heart, overproduce a secreted hormone, or induce an immune response.

Therefore, investigators have focused on a number of strategies to circumvent these risks. *In vitro* positive selection of differentiated cells or negative selection of residual pluripotent cells prior to *in vivo* delivery is one possible approach to teratoma prevention, but does not address the other potential toxicities arising *in vivo*.<sup>31</sup> The introduction of suicide genes into pluripotent cells, allowing "on demand" ablation of cells *in vitro* prior to delivery or *in vivo* in case of toxicity is a very attractive strategy. Utilization of a pluripotent-specific promoter could allow selective ablation of residual iPSC or ESC while sparing desirable differentiated cells, however, a strong constitutive promoter could be useful at least in initial safety studies to kill any iPSC-derived tissue *in vivo* in the setting of more general toxicity.

In this study, we have focused on the iCasp9 suicide gene activated to induce apoptosis by the nontoxic chemical inducer of dimerization AP1903. One prior report demonstrated that constitutive expression of the iCasp9 suicide gene from a strong retroviral promoter/enhancer (SFFV) within a lentiviral vector in nonhuman primate iPSC conferred efficient killing upon CID exposure *in vitro*, however *in vivo* activity was not explored.<sup>19</sup> We compared suicide gene efficiency and specificity of killing with three different promoters, the constitutive viral promoter CMV, the constitutive human promoter EF1 $\alpha$ , and finally the EOS-C(3+) promoter designed to have specificity for expression in pluripotent stem cells.<sup>37</sup> CMV is a widely used constitutive promoter which has been used to express many ectopic transgenes in mammalian cells,<sup>38,39</sup> including conferring GCV sensitivity to HSV-TK transduced murine ESC implanted in the central nervous system or flanks of immunodeficient mice.<sup>16</sup> But transgene expression driven by the CMV promoter has been found to be erratic and silenced in both immature and differentiated cell types.<sup>40-42</sup> In our studies, the CMV promoter was not sufficient for efficient iCasp9-mediated killing even *in vitro*, and the transgenes driven by this promoter were silenced in miPSC. The human EF1 $\alpha$  promoter has been described to be less prone to silencing and able to provide more stable long-term expression, while also less likely to activate adjacent proto-oncogenes via insertional mutagenesis than strong viral promoters such as SFFV.<sup>39,43,44</sup> For first time, we used the EF1 $\alpha$  promoter to drive expression of a suicide gene in pluripotent stem cells, expressing iCasp9 from this promoter in both miPSCs and RhiPSCs. EF1 $\alpha$ -iCasp9 was stably expressed in iPSCs *in vitro*, and also in the iPSC parental fibroblast cells. The EF1 $\alpha$ -iCasp9-transduced iPSCs were efficiently and rapidly killed by exposure to AP1903 *in vitro*. *In vitro* AP1903 pretreated EF1 $\alpha$ -iCasp9 iPSCs had significantly delayed tumor formation when administered to mice: 50% of the recipient mice remained teratoma-free at up to 400 days. This result suggests that *in vitro* purging of residual undifferentiated ES/iPSC using iCasp9/AP1903 is a potential efficient approach to reduce the potential *in vivo* tumorigenicity risk of pluripotent cells. However, *in vitro* purging would require utilization of a pluripotent-specific promoter instead of EF1 $\alpha$ .

The putative stem cell-specific promoter EOS-C(3+)<sup>37</sup> was not effective in our model either in terms of efficacy or specificity. *In vitro* AP1903 treatment did not result in complete killing, even at high concentrations. Moreover, the EOS-C(3+)-iCasp9 construct was also expressed in rhesus MSC and skin fibroblasts, conferring significant AP1903 killing even in these more differentiated cells. Taken together, these results suggest that other putative pluripotent stem cell specific promoters may be more effective. Other groups have shown that the *Nanog* or *Oct4* promoters may be effective in conferring ESC/iPSC-specific suicide gene expression, although to date these were only investigated in *in vitro*.<sup>18</sup> Another group utilized targeting to insert herpes TK into the endogenous *Oct4* locus, but found these lines were not sensitive to GCV.<sup>45</sup>

In our model, stability of iCasp9 suicide gene expression was an issue, particularly *in vivo* and with differentiation. EF1 $\alpha$ -iCasp9 was stably expressed in iPSC or stromal cells at steady state, and expression was stable when we reprogrammed EF1 $\alpha$ -iCasp9-transduced rhesus fibroblasts to EF1 $\alpha$ -iCasp9-RhiPSC, but EF1 $\alpha$ -iCasp9 expression was downregulated/silenced during iPSC differentiation *in vitro* and with teratoma formation *in vivo*. The EF1 $\alpha$ -iCasp9 downregulation seemed to be cell type-dependent. These results suggest that this property could be taken advantage of, if differentiated cells stop expressing the EF1 $\alpha$ -iCasp9 transgene, then potentially AP1903 could be used for purging of residual undifferentiated cells



*in vitro* prior to transplantation. However, to ablate teratomas *in vivo*, more stable or higher-expressing promoters may be required. Since iCasp9 is not an enzyme and must be actively incorporated into a macromolecular complex to induce apoptosis, high levels of gene expression are important for efficient killing. One study reported that phosphoglycerate kinase (PGK) or SFFV promoters could drive sufficient stable suicide gene expression in monkey iPSCs to allow *in vivo* teratoma ablation utilizing the yeast cytosine deaminase-5FU suicide gene system.<sup>19</sup>

We demonstrated that silencing of the lentiviral EF1 $\alpha$ -iCasp9 construct may be due to promoter DNA methylation, and that expression could be partly restored by treatment with 5-azacytidine, a demethylating agent. However, while day 17 EBs had even lower transgene protein expression as quantified by flow cytometry for the h $\Delta$ CD19 marker gene, despite relatively preserved mRNA expression, indicating that there might be some other mechanisms other than promoter methylation contributing to insufficient expression of the suicide gene at the protein level. Understanding the mechanisms of inactivation and reactivation of EF1 $\alpha$  promoter-controlled iCasp9 or other suicide transgenes during the differentiation process should help further develop effective strategies for therapeutic or suicide-gene expression in iPSC-derived differentiated cell products. Pfaff *et al.* recently reported that a ubiquitous chromatin opening element prevents transgene silencing in pluripotent stem cells and their differentiated progeny, which may be a useful approach to circumvent differentiation-induced transgene silencing during the generation of advanced iPSC/ESC-based gene and cell therapy products.<sup>46</sup>

In conclusion, in this study, we studied not only the cell death-switch capacity of the iCasp9/ AP1903 suicide system, but also investigated the feasibility of two ubiquitous promoters (EF1 $\alpha$  and CMV) and a pluripotent-specific promoter (EOS-C(3+)) to control suicide gene efficiency and specificity in iPSC and their differentiated progeny *in vitro* and *in vivo*. The development of more sensitive inducible caspase suicide genes is ongoing, and may facilitate ablation without requiring high expression. These suicide genes are really the only practical choices for clinical development at present, since all other current suicide gene systems contain yeast, bacterial or viral expressed proteins, and are likely to be immune targets and not compatible with long-term *in vivo* persistence in iPSC-derived tissues or organs. Use of nonviral and/or targeted systems for introduction of suicide genes and corrective genes is likely to be utilized for most clinical applications in the future, and analysis of the level of transgene expression as well as silencing may be more or less of an issue with these newer gene delivery approaches.

## MATERIALS AND METHODS

### Vector construction and viral transduction

The pCDH-iCasp9-2A-h $\Delta$ CD19 lentiviral vector contains a CMV promoter driving 2A-linked dual transgene expression and was provided by Gianpietro Dotti. To construct the EF1 $\alpha$ -iCasp9 and EOS-C(3+)-iCasp9 lentiviral vectors, the pCDH-iCasp9-2A-h $\Delta$ CD19 plasmid was digested with Xba1, the ends were processed with *Pfu* DNA polymerase to create blunt ends, and then digested with Cla1 to remove the CMV promoter. EF1 $\alpha$  and EOS-C(3+) promoter cassettes were amplified from PL-sin-EF1 $\alpha$ -EGFP and PL-SIN-EOS-C(3+)-EGFP plasmids using forward primers containing a Cla1 site and reverse primers with EcoRV site. The PCR products were digested with Cla1 and EcoRV then ligated with the promoterless vector backbone to generate EF1 $\alpha$ -iCasp9 and EOS-C(3+)-iCasp9 lentiviral vector plasmids. The EF1 $\alpha$  promoter is 1,176 bp and contains the first intron. The sequence of the promoter region in each vector was confirmed. Figure 1a shows schematic maps of each vector. The primers used for cloning and PCR are listed in Supplementary Table S1.

EF1 $\alpha$ -iCasp9-h $\Delta$ CD19, EOS-C(3+)-iCasp9-h $\Delta$ CD19 and CMV-iCasp9-h $\Delta$ CD19 lentiviral vector particles were produced by calcium-phosphate transfection of 293T cells with the vector and helper plasmids as previously described.<sup>47</sup> Functional particle titer was determined by limit dilution transduction of HeLa cells followed by flow cytometry for h $\Delta$ CD19 expression using an anti-human CD19 antibody (clone 4G7, BD Biosciences, San Jose, CA). Apolycistronic STEMCCA-OSKM lentiviral vector expressing the transcription factors *POU5F1*, *SOX2*, *KLF4*, and *cMYC* was utilized to generate rhesus macaque iPSC as described.<sup>6,48</sup>

### Cell culture

miPSC were maintained in an undifferentiated pluripotent state in ES medium consisting of Dulbecco's modified Eagle's medium (DMEM) supplemented with 15% (v/v) fetal bovine serum, 0.1 mmol/l  $\beta$ -mercaptoethanol, 1% nonessential amino acids, 100 IU/ml penicillin, 100 mg/ml streptomycin, 4 mmol/l L-glutamine, and 1,000 IU/ml leukemia inhibitory factor (LIF) (Millipore, Billerica, MA). Cells were grown on feeder layers of irradiated murine embryonic fibroblasts (MEFs) and were split every 2–3 days by trypsinization.

Rhesus skin fibroblast cells were derived from abdominal skin biopsies, and cultured in DMEM with 10% FBS, 100 IU/ml penicillin, 100 mg/ml streptomycin, and 4 mmol/l L-glutamine. RhiPSC were cultured in knock-out DMEM supplemented with 20% knockout serum (Life Technologies, Grand Island, NY), 0.1 mmol/l  $\beta$ -mercaptoethanol, 1% nonessential amino acids, 100 IU/ml penicillin, 100 mg/ml streptomycin, 4 mmol/l L-glutamine, and 20 ng/ml Fibroblast Growth Factor-basic (bFGF) (PeproTech, Rocky Hill, NJ). Cells were grown on feeder layers of irradiated MEFs and were passaged every 5–7 days by manual splitting, without trypsin.

### Generation of rhesus and murine iCasp9-expressing iPSC cells

miPSC were generated from GFP-transgenic mouse (Strain: C57Bl/6-Tg (UBC-GFP) 30Scha/J (Jax # 004353)) tail fibroblasts by standard techniques, via retroviral transduction with four vectors expressing four mouse transcription factors (*POU5F1*, *SOX2*, *KLF4*, and *cMYC*) as described previously.<sup>1</sup> Following 2–3 weeks culture in ES media, morphologically-pluripotent colonies were isolated and expanded, and pluripotency documented by Alkaline Phosphatase (AP) staining (Sigma-Aldrich), SSEA-1 (anti-mouse SSEA-1, Stemgent, San Diego, CA) staining and teratoma formation in immunodeficient NOD scid gamma c (NSG, NOD.Cg-Prkdcscid Il2rgtm1Wjl/SzJ) mice. Lentiviral vectors expressing iCasp9 from different promoters were used to transduce miPSC to generate iCasp9 miPSC. For transduction, miPSC were dissociated into single cells with trypsin and plated onto 0.1% gelatin coated plates, and vector was added 24 hours later. Forty-eight hours following transduction, the cells were live-stained with anti-human CD19-PE, and h $\Delta$ CD19 positive clones were picked and expanded.

To generate RhiPSC, rhesus skin fibroblasts were transduced with the EF1 $\alpha$ -iCasp9 lentiviral vector, and 72 hours after transduction, the cells were stained with an anti-CD19-PE antibody and h $\Delta$ CD19+ cells were enriched using anti-PE microbeads (Miltenyi Biotec, Auburn, CA). iCasp9-h $\Delta$ CD19 positive fibroblasts were then reprogrammed using the STEMCCA-OSKM lentivirus to generate RhiPSC as described.<sup>6</sup> The pluripotency of iCasp9 RhiPSC cells was demonstrated via SSEA-4 (anti-SSEA-4, clone: MC813-70, BD Biosciences, San Jose, CA) staining, *in vitro* EB formation and *in vivo* teratoma formation in NSG mice. Murine and rhesus iPSC utilized were documented to have a normal karyotype via standard G-banding.

### *In vitro* AP1903 cytotoxicity assay

iCasp9 iPSCs were plated in six-well plates at  $0.5 \times 10^6$  per well. Twenty-four hours later, 0–100 nmol/l of the CID AP1903 (AP1903: 5 mg/ml stock, Bellicium Pharmaceuticals, Houston, TX) in fresh medium was added to the wells. Cells were analyzed morphologically via microscopy 4, 24, or 48 hours later, the cell viability was accessed by Annexin V/7-AAD apoptosis detection analysis (BD Biosciences, San Jose, CA).

### Teratoma assays and *in vivo* AP1903 treatment

All animals used in this study were housed and handled in accordance with protocols approved by the Animal Care and Use Committee of the National Heart, Lung and Blood Institute (H-0253). Female or male immune-deficient NSG aged 4–8 weeks were used for teratoma assays. miPSCs (3 million) or RhiPSCs ( $1 \times 10^7$  cells) were suspended in IMDM, mixed with Matrigel (BD

Biosciences, Bedford, MA) in a 1:1 ratio and then injected in a volume of 200–300  $\mu$ l subcutaneously or 100  $\mu$ l intramuscularly. Per the protocol, euthanasia was required with development of a tumor mass of greater than 2 cm diameter. AP9013 1–5 mg/kg was administered intravenously to the animals as a single dose or daily for 5 days, beginning either on the day of iPSC implantation, or 1 week later. For the intravenous miPSC teratoma mouse model, three million iPSC were suspended in 200  $\mu$ l IMDM without matrigel, and injected via the tail vein, and mice were euthanized when in respiratory distress. Tissues from the mice at the endpoint were fixed in Bouin's solution (Sigma-Aldrich) for histologic analysis. GFP+ growths were visualized by the Carestream Xtreme live animal imaging system (Carestream Health, Rochester, NY).

### Immunohistochemistry for evaluation of vessel formation

Evaluation of vessel formation in teratoma by CD31 immunostaining was performed on 3  $\mu$ m fixed paraffin-embedded tissue sections. The dewaxed and rehydrated slides were subjected to antigen retrieval in a microwave using a pressure cooker with 10 mmol/l Citrate buffer (pH 6.0) (K.D. Medical, Columbia, MD). It followed 15 minutes blocking with 3% Tris goat serum and incubation for 1 hour with primary CD31 antibody against CD31 (Abcam, ab28364) at concentration 1:100. EnVision FLEX rabbit kit (Dako, Carpinteria, CA) was used for detection. Human lung section was included as positive controls for antibody staining.

### EB formation and RhiPSC-derived MSC differentiation

Undifferentiated RhiPSC were harvested using a cell scraper and incubated in EB formation medium (RhiPSC medium without bFGF) for up to 17 days. The medium was replaced with fresh medium every 4–5 days. To analyze h $\Delta$ CD19 expression on EBs by flow cytometry, EBs was trypsinized (Life Technologies) into a single cell suspension. RhiPSC derived MSC differentiation was carried out as previously described.<sup>6</sup>

### PCR, RT-PCR, and qRT-PCR

DNA and RNA were purified using the DNeasy Blood & Tissue Kit or the RNeasyPlus Mini Kit (all Qiagen, Valencia, CA), respectively. cDNA was generated from RNA using the SuperScript III First-Strand Synthesis System (Life Technologies). Promoter specific PCR was performed on genomic DNA of different promoter iPSC clones to confirm the vectors were transduced into the cells. Promoter specific qRT-PCR was performed to determine iCasp9 expression levels in iPSCs, iPSC derived MSCs, EBs and teratoma tissue. All primers are listed in Supplementary Table S1.

### Quantification of CpG methylation of the EF1 $\alpha$ promoter by pyrosequencing

Bisulfite conversion and pyrosequencing of the EF1 $\alpha$  promoter region was performed using the EpigenDx (Hopkinton, MA) system. Briefly, 500 ng of genomic DNA underwent bisulfate conversion and purification and 25 ng of purified bisulfate-converted DNA was used for each methylation specific PCR. 10  $\mu$ l of the PCR products were sequenced by using the pyrosequencing PSQ96 HS System (Biotage, AB) following the manufacturer's instructions (Pyrosequencing, Qiagen). The methylation status of each locus was analyzed individually as a T/C SNP using QCpG software (Pyrosequencing, Qiagen). The human EF1 $\alpha$  promoter CpG Island prediction mapping was done using the online tool from the Li Lab in the Department of Urology, UCSF (<http://www.urogene.org/cgi-bin/methprimer/methprimer.cgi>).

### Statistical analysis

Survival analysis was performed according to the "Log-rank (Mantel-Cox) Test" and the Kaplan–Meier plots to present survival curves (GraphPad Prism 5).  $P < 0.05$  was considered as statistically significant.

### ACKNOWLEDGMENTS

This work was supported by intramural funding from the National Heart, Lung, and Blood Institute (NHLBI) and the National Center for Regenerative Medicine (NCRM). We thank Jichun Chen and Marie Desierto from the Hematology Branch, and ZuXi Yu from the NHLBI pathology core facility for their assistance with teratoma assays, and Vivian Diaz from NIH Mouse Imaging Facility (MIF) for GFP live cell imaging. We thank

Gianpietro Dotti for providing the pCDH-iCasp9-2A-h $\Delta$ CD19 lentiviral vector. D.M.S. is employed by Bellicum Pharmaceuticals. The other authors declare no conflict of interest.

### REFERENCES

- Takahashi, K and Yamanaka, S (2006). Induction of pluripotent stem cells from mouse embryonic and adult fibroblast cultures by defined factors. *Cell* **126**: 663–676.
- Takahashi, K, Tanabe, K, Ohnuki, M, Narita, M, Ichisaka, T, Tomoda, K *et al.* (2007). Induction of pluripotent stem cells from adult human fibroblasts by defined factors. *Cell* **131**: 861–872.
- de Peppo, GM and Marolt, D (2012). State of the art in stem cell research: human embryonic stem cells, induced pluripotent stem cells, and transdifferentiation. *J Biol Transfus* **2012**: 317632.
- Hanna, J, Wernig, M, Markoulaki, S, Sun, CW, Meissner, A, Cassady, JP *et al.* (2007). Treatment of sickle cell anemia mouse model with iPS cells generated from autologous skin. *Science* **318**: 1920–1923.
- Lu, TY, Lin, B, Kim, J, Sullivan, M, Tobita, K, Salama, G *et al.* (2013). Repopulation of decellularized mouse heart with human induced pluripotent stem cell-derived cardiovascular progenitor cells. *Nat Commun* **4**: 2307.
- Hong, SG, Winkler, T, Wu, C, Guo, V, Pittaluga, S, Nicolae, A *et al.* (2014). Path to the clinic: assessment of iPSC-based cell therapies *in vivo* in a nonhuman primate model. *Cell Rep* **7**: 1298–1309.
- Kuroda, T, Yasuda, S and Sato, Y (2013). Tumorigenicity studies for human pluripotent stem cell-derived products. *Biol Pharm Bull* **36**: 189–192.
- Ben-David, U and Benvenisty, N (2011). The tumorigenicity of human embryonic and induced pluripotent stem cells. *Nat Rev Cancer* **11**: 268–277.
- Blum, B and Benvenisty, N (2008). The tumorigenicity of human embryonic stem cells. *Adv Cancer Res* **100**: 133–158.
- Ciceri, F, Bonini, C, Gallo-Stampino, C and Bordignon, C (2005). Modulation of GvHD by suicide-gene transduced donor T lymphocytes: clinical applications in mismatched transplantation. *Cytotherapy* **7**: 144–149.
- Barese, CN, Krouse, AE, Metzger, ME, King, CA, Traversari, C, Marini, FC *et al.* (2012). Thymidine kinase suicide gene-mediated ganciclovir ablation of autologous gene-modified rhesus hematopoiesis. *Mol Ther* **20**: 1932–1943.
- Bonini, C, Bondanza, A, Perna, SK, Kaneko, S, Traversari, C, Ciceri, F *et al.* (2007). The suicide gene therapy challenge: how to improve a successful gene therapy approach. *Mol Ther* **15**: 1248–1252.
- Dachs, GU, Hunt, MA, Syddall, S, Singleton, DC and Patterson, AV (2009). Bystander or no bystander for gene directed enzyme produg therapy. *Molecules* **14**: 4517–4545.
- Maily, L, Leboeuf, C, Tiberghien, P, Baumert, T and Robinet, E (2010). Genetically engineered T-cells expressing a ganciclovir-sensitive HSV-tk suicide gene for the prevention of GvHD. *Curr Opin Investig Drugs* **11**: 559–570.
- Schuldiner, M, Itskovitz-Eldor, J and Benvenisty, N (2003). Selective ablation of human embryonic stem cells expressing a "suicide" gene. *Stem Cells* **21**: 257–265.
- Jung, J, Hackett, NR, Pergolizzi, RG, Pierre-Destine, L, Krause, A and Crystal, RG (2007). Ablation of tumor-derived stem cells transplanted to the central nervous system by genetic modification of embryonic stem cells with a suicide gene. *Hum Gene Ther* **18**: 1182–1192.
- Cheng, F, Ke, Q, Chen, F, Cai, B, Gao, Y, Ye, C *et al.* (2012). Protecting against wayward human induced pluripotent stem cells with a suicide gene. *Biomaterials* **33**: 3195–3204.
- Chen, F, Cai, B, Gao, Y, Yuan, X, Cheng, F, Wang, T *et al.* (2013). Suicide gene-mediated ablation of tumor-initiating mouse pluripotent stem cells. *Biomaterials* **34**: 1701–1711.
- Zhong, B, Watts, KL, Gori, JL, Wohlfahrt, ME, Ennsle, J, Adair, JE *et al.* (2011). Safeguarding nonhuman primate iPSC cells with suicide genes. *Mol Ther* **19**: 1667–1675.
- Bonini, C, Ferrari, G, Verzeletti, S, Servida, P, Zappone, E, Ruggieri, L *et al.* (1997). HSV-TK gene transfer into donor lymphocytes for control of allogeneic graft-versus-leukemia. *Science* **276**: 1719–1724.
- Ciceri, F, Bonini, C, Stanghellini, MT, Bondanza, A, Traversari, C, Salomoni, M *et al.* (2009). Infusion of suicide-gene-engineered donor lymphocytes after family haploidentical haemopoietic stem-cell transplantation for leukaemia (the TK007 trial): a non-randomised phase I-II study. *Lancet Oncol* **10**: 489–500.
- Fareed, MU and Moolten, FL (2002). Suicide gene transduction sensitizes murine embryonic and human mesenchymal stem cells to ablation on demand—a fail-safe protection against cellular misbehavior. *Gene Ther* **9**: 955–962.
- Menzel, O, Birraux, J, Wildhaber, BE, Jond, C, Lasne, F, Habre, W *et al.* (2009). Biosafety in ex vivo gene therapy and conditional ablation of lentivirally transduced hepatocytes in nonhuman primates. *Mol Ther* **17**: 1754–1760.
- Lim, TT, Geisen, C, Hesse, M, Fleischmann, BK, Zimmermann, K and Pfeifer, A (2013). Lentiviral vector mediated thymidine kinase expression in pluripotent stem cells enables removal of tumorigenic cells. *PLoS ONE* **8**: e70543.
- Berger, C, Flowers, ME, Warren, EH and Riddell, SR (2006). Analysis of transgene-specific immune responses that limit the *in vivo* persistence of adoptively transferred HSV-TK-modified donor T cells after allogeneic hematopoietic cell transplantation. *Blood* **107**: 2294–2302.

26. Garin, MI, Garrett, E, Tiberghien, P, Apperley, JF, Chalmers, D, Melo, JV et al. (2001). Molecular mechanism for ganciclovir resistance in human T lymphocytes transduced with retroviral vectors carrying the herpes simplex virus thymidine kinase gene. *Blood* **97**: 122–129.
27. Di Stasi, A, Tey, SK, Dotti, G, Fujita, Y, Kennedy-Nasser, A, Martinez, C et al. (2011). Inducible apoptosis as a safety switch for adoptive cell therapy. *N Engl J Med* **365**: 1673–1683.
28. Spencer, DM, Wandless, TJ, Schreiber, SL and Crabtree, GR (1993). Controlling signal transduction with synthetic ligands. *Science* **262**: 1019–1024.
29. Fan, L, Freeman, KW, Khan, T, Pham, E and Spencer, DM (1999). Improved artificial death switches based on caspases and FADD. *Hum Gene Ther* **10**: 2273–2285.
30. Straathof, KC, Pulè, MA, Yotnda, P, Dotti, G, Vanin, EF, Brenner, MK et al. (2005). An inducible caspase 9 safety switch for T-cell therapy. *Blood* **105**: 4247–4254.
31. Kiuru, M, Boyer, JL, O'Connor, TP and Crystal, RG (2009). Genetic control of wayward pluripotent stem cells and their progeny after transplantation. *Cell Stem Cell* **4**: 289–300.
32. Lawrenz, B, Schiller, H, Willbold, P, Ruediger, M, Muhs, A and Esser, S (2004). Highly sensitive biosafety model for stem-cell-derived grafts. *Cytotherapy* **6**: 212–222.
33. Fujikawa, T, Oh, SH, Pi, L, Hatch, HM, Shupe, T and Petersen, BE (2005). Teratoma formation leads to failure of treatment for type I diabetes using embryonic stem cell-derived insulin-producing cells. *Am J Pathol* **166**: 1781–1791.
34. Darabi, R, Gehlbach, K, Bachoo, RM, Kamath, S, Osawa, M, Kamm, KE et al. (2008). Functional skeletal muscle regeneration from differentiating embryonic stem cells. *Nat Med* **14**: 134–143.
35. Amariglio, N, Hirshberg, A, Scheithauer, BW, Cohen, Y, Loewenthal, R, Trakhtenbrot, L et al. (2009). Donor-derived brain tumor following neural stem cell transplantation in an ataxia telangiectasia patient. *PLoS Med* **6**: e1000029.
36. Hong, SG, Dunbar, CE and Winkler, T (2013). Assessing the risks of genotoxicity in the therapeutic development of induced pluripotent stem cells. *Mol Ther* **21**: 272–281.
37. Hotta, A, Cheung, AY, Farra, N, Vijayaragavan, K, Séguin, CA, Draper, JS et al. (2009). Isolation of human iPSC cells using EOS lentiviral vectors to select for pluripotency. *Nat Methods* **6**: 370–376.
38. Yang, X, Boehm, JS, Yang, X, Salehi-Ashtiani, K, Hao, T, Shen, Y et al. (2011). A public genome-scale lentiviral expression library of human ORFs. *Nat Methods* **8**: 659–661.
39. Mao, G, Marotta, F, Yu, J, Zhou, L, Yu, Y, Wang, L et al. (2008). DNA context and promoter activity affect gene expression in lentiviral vectors. *Acta Biomed* **79**: 192–196.
40. Doerfler, W, Hoeveler, A, Weisshaar, B, Dobrzanski, P, Knebel, D, Langner, KD et al. (1989). Promoter inactivation or inhibition by sequence-specific methylation and mechanisms of reactivation. *Cell Biophys* **15**: 21–27.
41. Duan, B, Cheng, L, Gao, Y, Yin, FX, Su, GH, Shen, QY et al. (2012). Silencing of fat-1 transgene expression in sheep may result from hypermethylation of its driven cytomegalovirus (CMV) promoter. *Theriogenology* **78**: 793–802.
42. Choi, KH, Basma, H, Singh, J and Cheng, PW (2005). Activation of CMV promoter-controlled glycosyltransferase and beta-galactosidase glycoconjugates by butyrate, tricostatin A, and 5-aza-2'-deoxycytidine. *Glycoconj J* **22**: 63–69.
43. Škalamera, D, Dahmer, M, Purdon, AS, Wilson, BM, Ranall, MV, Blumenthal, A et al. (2012). Generation of a genome scale lentiviral vector library for EF1a promoter-driven expression of human ORFs and identification of human genes affecting viral titer. *PLoS ONE* **7**: e51733.
44. Cesana, D, Ranzani, M, Volpin, M, Bartholomae, C, Duros, C, Artus, A et al. (2014). Uncovering and dissecting the genotoxicity of self-inactivating lentiviral vectors in vivo. *Mol Ther* **22**: 774–785.
45. Ou, W, Li, P and Reiser, J (2013). Targeting of herpes simplex virus 1 thymidine kinase gene sequences into the OCT4 locus of human induced pluripotent stem cells. *PLoS ONE* **8**: e81131.
46. Pfaff, N, Lachmann, N, Ackermann, M, Kohlscheen, S, Brendel, C, Maetzig, T et al. (2013). A ubiquitous chromatin opening element prevents transgene silencing in pluripotent stem cells and their differentiated progeny. *Stem Cells* **31**: 488–499.
47. Wu, C, Jares, A, Winkler, T, Xie, J, Metais, JY and Dunbar, CE (2013). High efficiency restriction enzyme-free linear amplification-mediated polymerase chain reaction approach for tracking lentiviral integration sites does not abrogate retrieval bias. *Hum Gene Ther* **24**: 38–47.
48. Sommer, CA, Stadtfeld, M, Murphy, GJ, Hochedlinger, K, Kotton, DN and Mostoslavsky, G (2009). Induced pluripotent stem cell generation using a single lentiviral stem cell cassette. *Stem Cells* **27**: 543–549.



This work is licensed under a Creative Commons Attribution-NonCommercial-NoDerivs 3.0 Unported License. The images or other third party material in this article are included in the article's Creative Commons license, unless indicated otherwise in the credit line; if the material is not included under the Creative Commons license, users will need to obtain permission from the license holder to reproduce the material. To view a copy of this license, visit <http://creativecommons.org/licenses/by-nc-nd/3.0/>

Supplementary Information accompanies this paper on the *Molecular Therapy—Methods & Clinical Development* website (<http://www.nature.com/mtm>)